Available online at www.sciencedirect.com

ScienceDirect

Procedia Engineering 10 (2011) 3677–3682

Engineering Procedia

ICM11

Defect tolerance of a gamma titanium aluminide alloy

M. Filippini[a,*], S. Beretta[a], L. Patriarca[a], G. Pasquero[b], S. Sabbadini[b]

[a]*Politecnico di Milano, Dipartimento di Meccanica, Via La Masa 1, 20156 Milano, Italy*
[b]*Avio S.p.A., Via I Maggio, 99, 10040 Rivalta di Torino, Italy*

Abstract

The fatigue properties of a Ti-48Al-2Cr-2Nb alloy obtained by electron beam melting (EBM) with a patented process has been examined by conducting high cycle fatigue tests performed at different loading ratios at room temperature. Fatigue crack tests have been performed for the purpose of characterizing the fatigue crack growth rate and threshold of the material. In order to assess the sensitivity of the material to the presence of defects and to adopt suitable fatigue design criteria, fatigue tests with artificial defects have been also performed with different defect size and loading ratio. Fatigue tests have been interpreted by the adoption of a suitable model based on the small crack approach, highlighting individual fatigue characteristics of the studied TiAl alloy.

Keywords: gamma titanium aluminides; high cycle fatigue; fatigue crack propagation; short crack behavior.

1. Introduction

Gamma titanium aluminide based alloys have become an important contender for structural applications in the aircraft industry to replace current nickel-based superalloys as the material of choice for low-pressure turbine blades [1-2]. The advantages achieved by the use of γ-TiAl intermetallics are principally their low density (3.9-4.2 g/cm^3 as a function of their composition), high specific yield strength, high specific stiffness, substantial resistance to oxidation and good creep properties up to high temperatures. In particular, the lower density will contribute to significant engine weight savings and reduced stresses on rotating components such as low-pressure turbine blades [3]. Although such materials appears very promising for the turbine engine industry, optimizing the performance improvements requires more advanced approaches to accurately predict fatigue life. Therefore, there is a need to

* Corresponding author. Tel.: +39-02-2399-8220; fax: +39-02-2399-8202.
E-mail address: mauro.filippini@polimi.it.

Selection and peer-review under responsibility of ICM11 doi:10.1016/j.proeng.2011.04.605

understand and address the specific fatigue properties of these materials to assure adequate reliability of these alloys in structural applications [4]. Additionally, their intrinsic brittleness at low temperatures is a matter of concern for application in the highly loaded parts of gas turbine engines. Moreover, it is difficult to obtain a component produced with γ-TiAl intermetallics with exactly the composition and microstructure desired. A further difficulty is that in the typical aeroengines applications must have an extremely low oxygen content, preferably much lower than 1500 ppm.

Electron beam melting (EBM) is a type of additive manufacturing for metal parts. It is often classified as a rapid manufacturing method. The technology manufactures parts by melting metal powder layer by layer with an electron beam in a high vacuum. Using EBM technology, the process of material production operates under high vacuum conditions, thereby reducing the risk of oxidation in the material of the final components. EBM technology for "layer by layer" productions offers several advantages with respect to other competing technologies and it is possible to operate at temperatures closer to the melting points of the intermetallic alloys [5]. In the EBM process, components are produced without vaporization of the powders of the initial material and the powders are made of an intermetallic alloy based on titanium and aluminium with the same chemical composition as the final intermetallic with which the components are produced.

2. Material and specimens geometry

2.1. Material

The gamma titanium aluminide (γ-TiAl) Ti-48Al-2Cr-2Nb alloy studied in this work has been produced according to a patented process [6] with EBM A2 machine produced and distributed by ARCAM AB (Sweden), which allows focused electron beam melting to be performed in high vacuum conditions. Material has been produced in the form of near net shape specimens and final specimens geometry was manufactured by conventional machining with carefully selected cutting parameters for removing the machining allowance.

2.2. Specimens

For the tests conducted in the present work, three different type of specimens have been produced. A set of 30 unnotched specimens suitable for high cycle fatigue testing have been produced with the geometry shown in Fig. 1.a. A smaller set of 6 specimens suitable for crack propagation testing have been produced with the geometry shown in Fig. 1.b). In all cases, prior to fatigue testing, the surface of the specimens has been pre-oxidized, by furnace treatment in air for 20 hr at a temperature of 650°C [7].

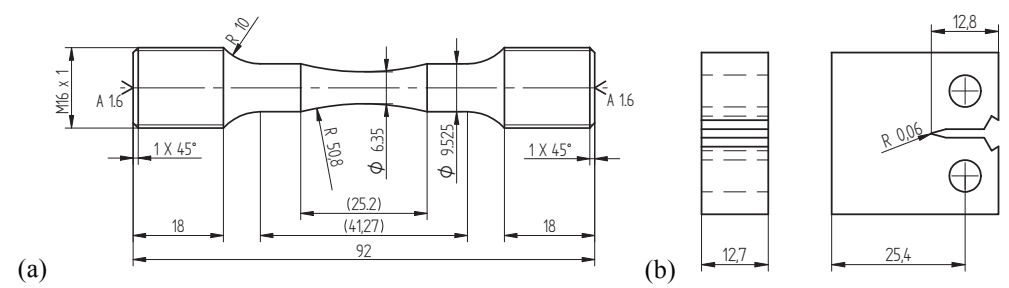

Fig. 1 Shape and dimensions of: (a) unnotched specimens employed for uniaxial fatigue testing; (b) fatigue crack propagation testing.

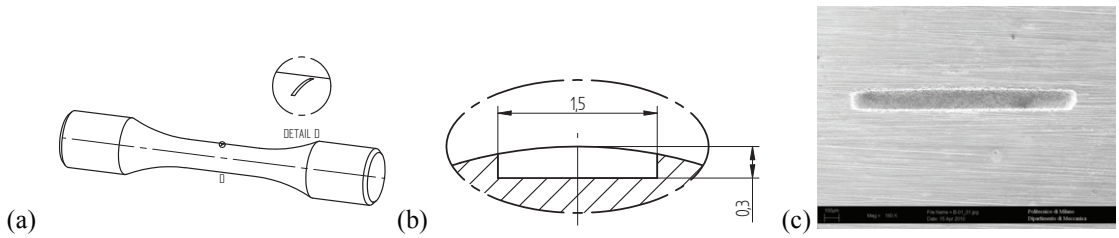

(a) (b) (c)

Fig. 2 (a) Geometry of specimens for assessing defect sensitivity in short crack fatigue testing (8 mm gauge dia); (b) nominal shape of artificial defect of √*area*=644 μm; (c) SEM picture of artificial defects produced by EDM.

Additionally, a set of 40 specimens with a gauge diameter of 8 mm have been produced and two type of artificial defects in the form of tiny rectangular micro-slots have been carefully produced in the mid section of the specimens by EDM, as shown in Fig. 2. Small artificial defects with dimensions of 500x100 μm (√area=220 μm) (not shown in Fig. 2) and larger artificial defects with dimensions of 1500x300 μm (√area=644 μm) have been introduced in the specimens, Fig. 2.

3. Test methods

3.1. Fatigue testing with plain specimens

Fatigue tests with plain axial specimens have been carried out at room temperature (RT) by employing the Rumul Testronic test system available at the laboratories of the Dipartimento di Meccanica of the Politecnico di Milano. Fatigue tests have been conducted by applying the staircase technique and the number of cycles of censored test (runout) has been fixed at 10^7 cycles. Tests have been carried out with three different loading ratio: i) $R=\sigma_{min}/\sigma_{max}=0$ (zero to tension); ii) $R= \sigma_{min}/\sigma_{max} =0.6$; iii) $R= \sigma_{min}/\sigma_{max} =-1$ (pure alternating stress).

3.2. Fatigue crack growth testing

Fatigue crack growth tests have been carried out in a servo-hydraulic MTS 810 testing machine and the crack length monitored by COD gage. The fracture mechanics specimens have been pre-cracked in cyclic compression. By pre-cracking specimens in cyclic compression, the effects of crack closure at the beginning of the real crack growth test is cancelled. For starting a crack in cyclic compression by small load amplitudes the wire EDM starter notch was sharpened by a razor blade polishing technique [8]. In order to determine the ΔK_{th} and the long crack propagation behaviour, FCG tests at room temperature have been carried out at constant R ratio (R=0.05 and R=0.6) by increasing the load amplitude in steps until the threshold value for a long crack is reached.

3.3. Fatigue testing with artificial defects

In order to generate small cracks at the root of the EDM notches, all specimens with artificial defects have been submitted to a pre-cracking procedure consisting of fatigue loading in cycling compression for a number of cycles up to 10^7. This procedure ensures that fatigue cracks are generated at the root of the EDM notch, by keeping at minimum compressive residual stresses at crack tip. After pre-cracking, all specimens have been pre-oxidized by furnace treatment in air for 20 hr at a temperature of 650°C, as in

the case of unnotched and FCG specimens. Finally, fatigue tests have been performed according to the staircase procedure at R=0 and R=0.6, with defects with √area equal to 220 μm and 644 μm, respectively.

4. Experimental results

4.1. Fatigue tests with plain specimens

The fatigue test results of the set carried out with plain specimens at R=0.6 are shown in Fig 3.a. In all the tests, it has been observed that, independently of the R ratio, the Wöhler curves are extremely flat. This means that a small variation in the applied stress amplitude can lead to substantial differences in the number of cycles to failure. The HCF test results obtained in the test campaign can be condensed in a single (Haigh) diagram, Fig 3.b. By comparing the tests results at different loading ratios in terms of maximum stress, it can be observed that the fatigue limit, in terms of maximum stress, is nearly independent of the loading ratio. In the diagram of Fig 3.b, the experimentally obtained fatigue limit values lie just below the dashed curve, representing the equation:

$$\sigma_{\max} = \sigma_m + \sigma_a = R_m \qquad (1)$$

where σ_m and σ_a represent the mean and alternating stress, respectively, while R_m is the ultimate tensile strength, obtained by tests in earlier tests. This specific behaviour has been observed also in the course of the test campaign, with nearly all specimen failing in the case the applied (maximum) stress was near or above the ultimate tensile strength, with no specimen failing (within 10^7 cycles) for maximum stress equal or below 320 MPa, irrespectively of the loading ratio R. The fracture surfaces analysed by SEM reveals that fatigue failures originate from lamellas that, due to their unfavourable direction respect to that of loading, determine a translamellar cleavage initial fracture, Fig. 3.c. These microstructural features has an average area of about 22000 μm^2, corresponding to an equivalent crack size of √area = 150 μm.

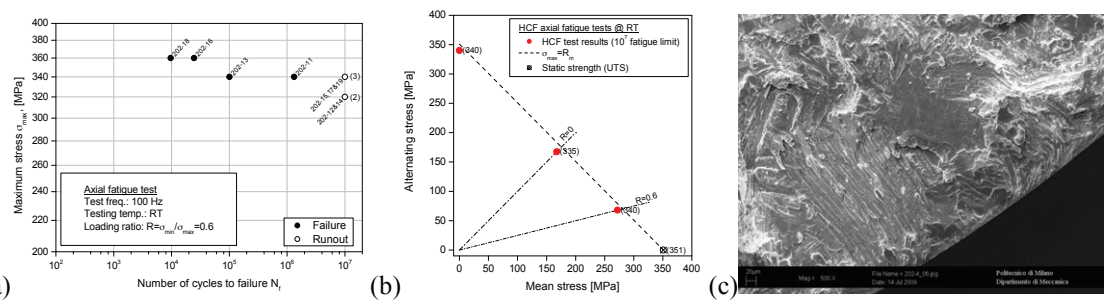

Fig. 3 Wöhler diagram of HCF test results at R=0.6 (a). Haigh diagram for the HCF tests with plain specimens (b). Typical failure initiation site found in fatigue tests: specimen failed after 3.2 10^6 cycles (R=0; Δσ=340 MPa).

4.2. Fatigue crack growth behavior

In the FCG tests a coherent behaviour was observed: for the tests conducted at R=0.05 no crack growth was observed for ΔK below 6 MPa√m, while for the tests at R=0.6, ΔK_{th} is about 3 MPa√m. The critical K_{max} value, corresponding to specimen failure, is in the range 10.5-11.5 MPa√m, independently of the applied R=K_{min}/K_{max} ratio. The FCG rate curves are shown in Fig. 4. The threshold values determined here are in accordance with those reported in literature for the lamellar microstructure of γ-TiAl

alloys [9]. It can be observed that the available ΔK range for crack growth is rather limited, due to the relatively limited difference between ΔK_{th} and K_{max}, resulting in high value of the slope. However, it must be observed that the γ-TiAl produced with the patented EBM process offer superior FCG characteristics respect to those of TiAl alloys obtained by conventional PM process [4,9].

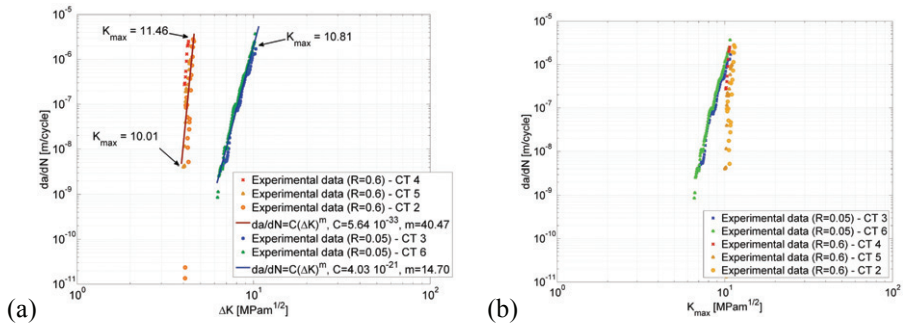

Fig. 4 Fatigue crack growth rate curves in terms of: a) ΔK, range of stress intensity factor; b) K_{max}.

4.3. Fatigue tests with artificial defects

By employing the Murakami model [10] for the assessment of the range of stress intensity factor (surface defects) as $\Delta K=0.65\Delta\sigma\,(\pi\sqrt{\text{area}})^{1/2}$, the threshold corresponding to the endurance strength for each R ratio can be evaluated. In the plots of Fig. 5, for loading ratio of R=0 and R=0.6, respectively, endurance strength stress ranges are given as a function of the equivalent defect size √area. Since it's been observed that the fatigue failures in plain specimens were found in correspondence of peculiar microstructural features with a typical size of $\sqrt{\text{area}_i}$=150 μm, the modification of the El-Haddad model by Tanaka [11] have been applied in the form:

$$\Delta\sigma_{th}=\Delta\sigma_e^i\sqrt{\frac{\sqrt{area}'_0}{\sqrt{area}+\sqrt{area}'_0-\sqrt{area}_i}}\quad\text{with}\quad\sqrt{area}'_0=\frac{1}{\pi}\left(\frac{\Delta K_{th}^{FCG}}{0.65\Delta\sigma_e^i}\right)^2=\sqrt{area}_0+\sqrt{area}_i \qquad (2)$$

where $\Delta\sigma^i_e$ represents the fatigue endurance strength obtained in the fatigue tests with plain specimens and a inherent defect $\sqrt{area_i}$ of 150 μm has been taken into account both for loading ratio R=0 and R=0.6.

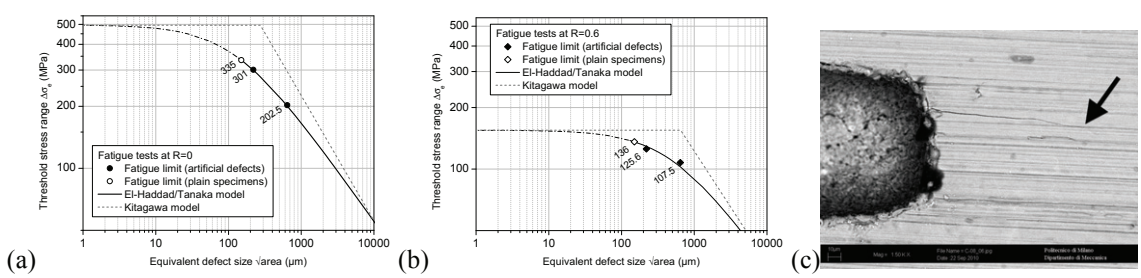

Fig. 5 Kitagawa diagram for: (a) loading ratio R=0; (b) loading ratio R=0.6. Slowly propagating fatigue cracks are observed in runout specimens (Δσ=300 MPa, R=0; 10^7 cycles without specimen failure), (c).

If a smaller volume of material would be stressed up to the threshold level, the probability of activating a inherent "microstructural" feature with size $\sqrt{area_i}$ is likely to become lower, i.e. the initial active defect size may be smaller for smaller stressed material volume. Theoretically, as the Kitagawa diagrams in Fig. 5 reveal, there is a possibility to observe an increased fatigue strength of the material when a non uniformly distributed loading is applied, as in the case of bending loading of thin sections. Additionally, it may be noted that the size of inherent microstructural features of 150 μm made in the present study is in the range of the colony dimensions, [12].

5. Conclusions

A potential disadvantage to cast and PM γ-TiAl alloys, in terms of component design, is their limited fatigue crack growth resistance and damage tolerance compared to nickel-based superalloys. In general, there is a small difference between the fatigue threshold stress-intensity-range of long cracks and the apparent fracture toughness, leading to shortened lifetimes for small changes in applied stress, should the fatigue threshold be exceeded. On the other hand, in the case of the Ti-48Al-2Cr-2Nb alloy examined in this work, the advantage of the γ-TiAl produced by the EBM process [6] is that typical defects of cast or PM materials can be avoided and higher fatigue threshold and fatigue strength respect to competing technologies can be obtained. From the observation of the test results the following conclusions may be drawn: the fatigue tests with artificial defects show that ΔK_{th} for defects larger than 100 μm can be described very accurately by a modified El-Haddad relationship; the values of the threshold stress intensity factor range depend on the loading ratio R, so that the mechanism does not seem to be governed by $K_{max.}$ only.

References

[1] Winstone, MR, Partridge, A, Brooks, JW. The contribution of advanced high-temperature materials to future aero-engines, *Proc. Instn Mech Eng L-J Mat*, 2001:**215**(L2): 63-73.

[2] Dimiduk, DM. Gamma titanium aluminide alloys - an assessment within the competition of aerospace structural materials. *Mat Sci Eng A-Struct*, 199:**263**(2): 281-8.

[3] Bartolotta P, Barrett J, Kelly T, Smashey R. The use of cast Ti-48Al-2Cr-2Nb in jet engines. *JOM, J. Min Met Mat Soc.*, 1997:**49**(5): 48-50,76.

[4] Henaff G. and Gloanec, A.-L., (2005). Fatigue properties of TiAl alloys. *Intermetallics*, **13**: 543-58.

[5] Murr LE, Gaytan SM, Ceylan A, Martinez E, Martinez JL, Hernandez DH, et al. Characterization of titanium aluminide alloy components fabricated by additive manufacturing using electron beam melting. *Acta Mater.*, 2010:**58**(5): 1887-94.

[6] Andersson L-E, Larsson M. Device and Arrangement for Producing a Three-Dimensional Object, Patent WO 01/81031 A1, 2001.

[7] Wu X, Huang A, Hu D, Loretto MH. Oxidation-induced embrittlement of TiAl alloys, *Intermetallics*, 2009:**17**(7): 540-52.

[8] Pippan R, Hageneder P, Knabl W, Clemens H, Hebesberger T, Tabernig B. Fatigue threshold and crack propagation in gamma-TiAl sheets. *Intermetallics*, 2001:**9**:89-96.

[9] Gloanec A-L, Henaff G, Bertheau D, Belaygue P, Grange M. Fatigue crack growth behaviour of a gamma-titanium-aluminide alloy prepared by casting and powder metallurgy. *Scripta Mater.*, 2003:**49**:825-30.

[10] Murakami Y. Metal Fatigue: Effect of Small Defects and Nonmetallic Inclusions. Oxford: Elsevier; 2002.

[11] Tanaka, K, Nakai, Y, Yamashita, M. Fatigue growth threshold of small cracks. *Int J Fracture*, 1981:17(5): 519-33.

[12] Voice, WE, Henderson, M.B, Shelton, EFJ, Wu, XH. Gamma titanium aluminide, TNB. *Intermetallics*, 2005:**13**(9), 959-64.